

## 1.5D internal multiple prediction on physical modeling data

Pan Pan, Kris Innanen and Joe Wong

### ABSTRACT

Multiple attenuation is a key aspect of seismic data processing, with the completeness of multiple removal often significantly affecting final image results. In this paper, we analyze 1.5D internal multiple prediction on physical modeling data simulating a 2D marine seismic survey designed to generate significant internal multiples. We describe a processing flow appropriate for preparation of the data for input into multiple prediction. Then we examine a 1.5D (i.e., pre-stack data over a layered geology) implementation of the inverse scattering series internal multiple prediction. The results show good agreement of predictions compared against synthetic data and physical modeling data. We discuss the selection of the integral limit parameter  $\epsilon$  and the influence of free-surface multiples. We also demonstrate that the beginning and ending integration points of frequencies, wavenumbers, and pseudo-depths in the code can be optimally chosen to reduce computational burden.

### INTRODUCTION

There are two advantages of the inverse scattering series internal multiple prediction method. First, this algorithm does not require any subsurface information. Secondly, first-order internal multiples are predicted with accurate times and approximate amplitudes. Internal multiple events are usually considered to be coherent noise in the seismic data. However, in many cases, internal multiples interfere with primary reflections, and removal of internal multiples without compromising primaries is very challenging in these cases. Reshef et al. (2003) pointed out that the prediction itself can be the final output, which is useful as an interpretation tool for identification only. Whether we decide to subtract them or not, the ability to identify internal multiples amongst primaries is still a technological necessity (Hernandez and Innanen, 2014).

In this paper, we discuss the acquisition, processing and multiple prediction analysis of a 2D common-source marine seismic survey. The purpose of this paper is to examine the response of the 1.5D internal multiple prediction algorithm as implemented in MATLAB on physical modeling data, and seek out an approach which can reduce computational burden and support interpretation. The data we acquired is designed to be strongly contaminated with internal multiples. After applying a processing flow on ProMax, we carry out a 1.5D internal multiple prediction, investigating its use on physical modeling data.

Seismic physical modeling provides scaled simulations of real world scenarios, the benefits of which are controlled acquisition geometry and physical model properties (Lawton et al., 1998). Physical modeling of seismic surveys has been conducted at the University of Calgary Seismic Physical Modeling Facility since 1985. Data are written into SEGY files, and gathers of seismograms can be read directly by processing packages such as ProMax (Wong et al., 2009a). Data are collected with a source transducer and a receiver transducer, each of which is moved independently by four linear motors

mounted on a gantry with digital position encoders and motor drives. Two of these motors are responsible for moving the gantry in the X direction, and the remaining two motors move the source or receiver transducer in the Y and Z direction. The eight motors on the two gantries are controlled through a desktop PC running the Windows XP system (Wong et al., 2009b). Additional details regarding the modeling systems are described by Lawton et al. (1989), and Wong et al. (2009a, 2009b).

## PHYSICAL MODELING EXPERIMENT

The first step to build a physical model is the selection of materials. The materials used in this case were water, PVC, Plexiglas and aluminum; the choice introduces several large impedance contrasts which induce significant internal multiples. We illustrate the schematic diagram of the physical modeling experiment in Figure 1, along with its scaled length and elastic parameters. The physical models were immersed into a tank of water.

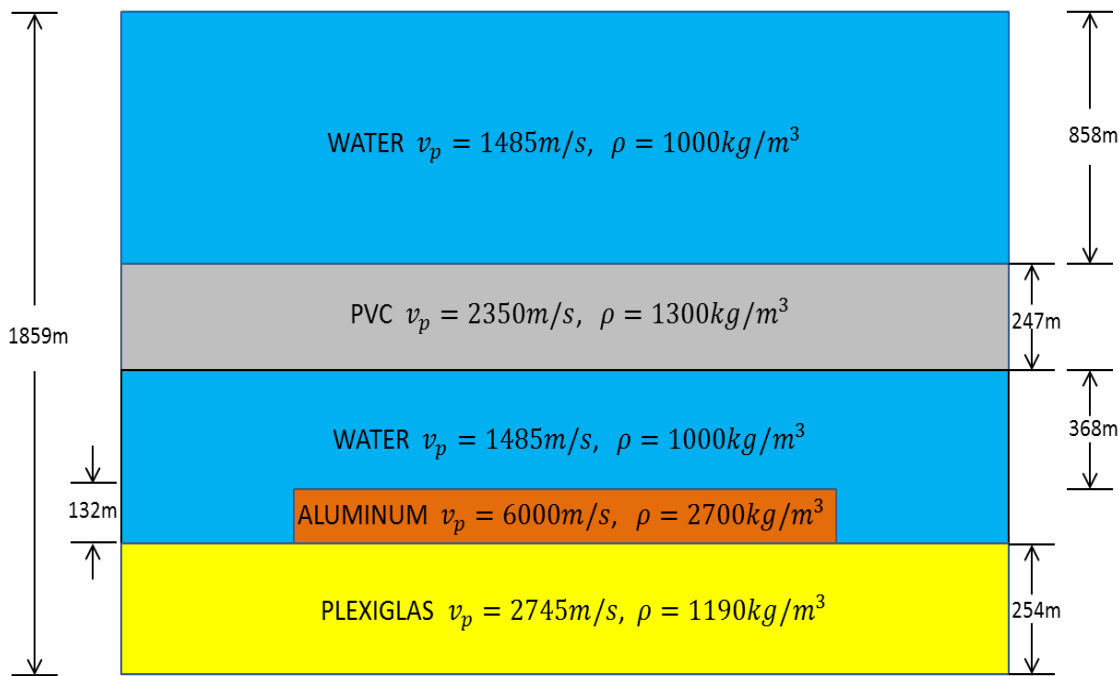


FIG. 1. Schematic diagram of the physical modeling experiment. All lengths are in scaled units (i.e., physical modeling units multiplied by 10000). The transducers are set just below the water surface.

We conducted a 2D common-source seismic survey over the model shown in Figure 1, with source fixed at a depth of 2mm below the water surface to avoid the source-ghost as much as possible. The source and receiver are 1.36mm-diameter piezoelectric CA-1136 pin transducers, acting as vertical component geophones. The source and receiver move in the Y direction along lines that are separated by 10mm in the X direction. The standard model scale factor is 1:  $10^4$ , so that 10mm in the model represents 100m in the real world, and 1 $\mu\text{s}$  represent 10ms. All measurement numbers in the report are scaled to represent field values and have approximate error of 5%. We move the receiver in the Y direction from left to right in increments of 25m, covering a total distance of 3.0km (Figure 2). A sample rate of 2ms was used during the acquisition. The scaled dominant frequencies of

the vibration pulse vary from 20 to 100Hz. In this study, we only consider the acoustic modeling.

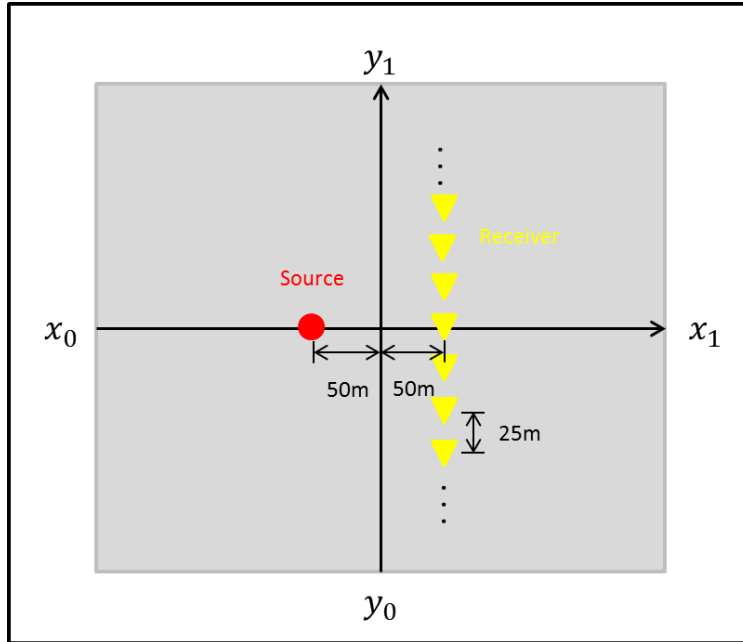


FIG. 2. Plan view of the physical modeling data acquisition. The source has been fixed, with the receiver moved from  $y_0$  to  $y_1$  direction in 25m increments and 121 traces were collected. All units are in field scale.

### SEISMIC DATA PROCESSING

We initially viewed the physical modeling data in Seisee for quality control, and then processed them using ProMax seismic data processing software. After some experimentation, a work flow has been created which is shown in Table 1.

Table 1. A processing flow applied to the physical modeling data.

	<b>PROCESSING FLOW</b>
1	Trace Header Math
2	Top Mute
3	Spiking Deconvolution
4	Bandpass Filter

The survey geometry was loaded from trace headers. From these basic headers, Trace Header Math was used to recreate the source and receiver coordinates to ensure that the data was in sequential order (Wong et al., 2009a). Then Trace Mute was applied to mute the energy of the direct wave. The raw data after Trace Mute is shown in Figure 3. In this figure, we can see that reverberations between the first two primaries are quite strong and must be repressed. Spiking deconvolution appears to be an effective tool for internal multiple prediction pre-processing, which shortens the period of the embedded source wavelet, trying to create a spike (Geldart and Sheriff, 2004). The operator length was

80ms and the operator prediction distance was 35ms. Predictive deconvolution was also investigated, however it seemed to repress the reverberations in the much later multiples (about 2300~2600ms). Since we wish to retain the energy of multiples, we avoided using predictive deconvolution. After performing filter panel tests, a bandpass filter of 15-20-70-90Hz was also applied. The deconvolved data is shown in Figure 4.

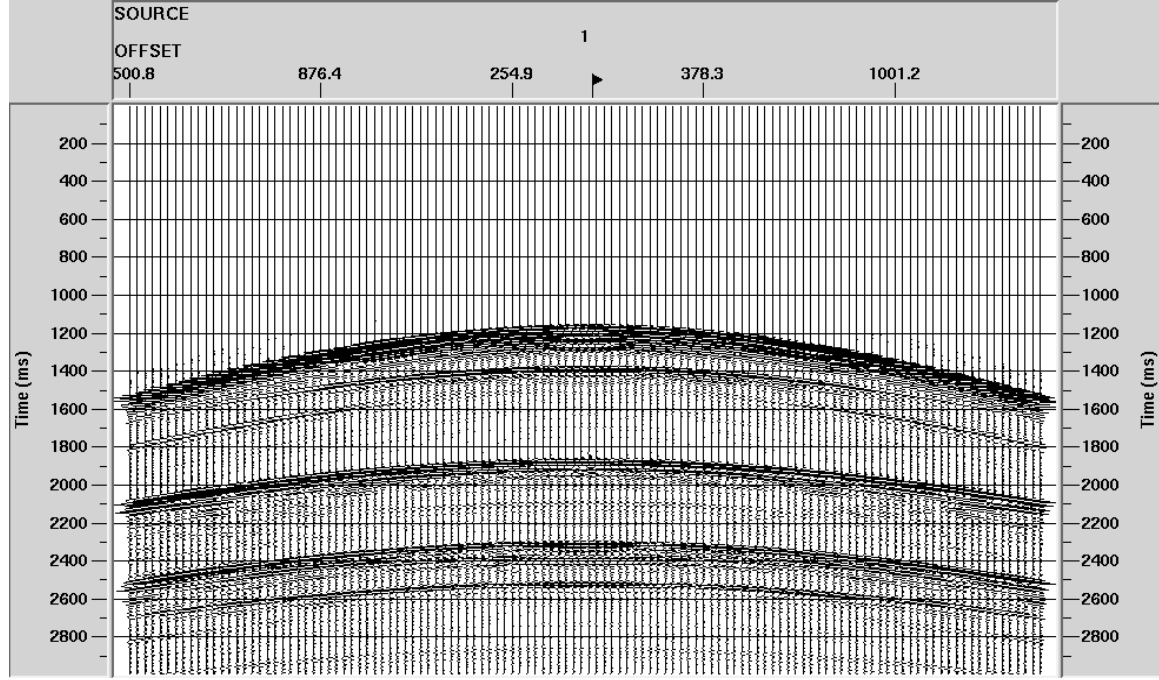


FIG. 3. Raw data after applying Trace Mute.

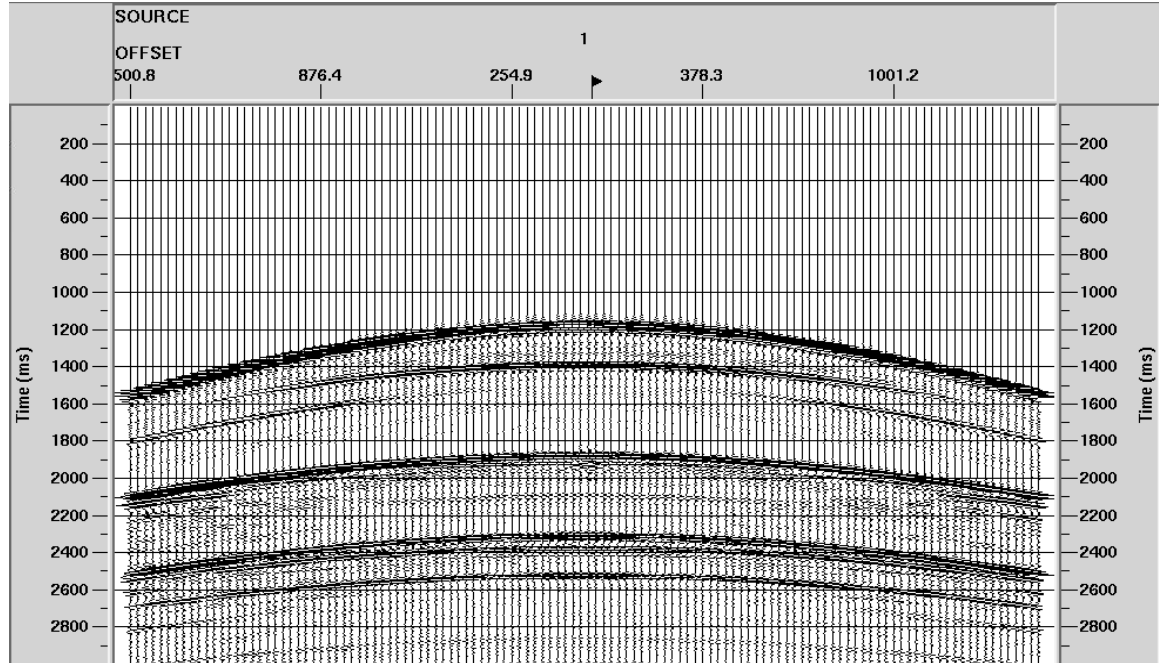


FIG. 4. The deconvolved data with decon operator length was 80ms and operator prediction distance was 35ms. A bandpass filter of 15-20-70-90Hz was also applied.

## 1.5D INTERNAL MULTIPLE PREDICTION

### Event identification

After pre-processing, we then analyzed our input using multiple prediction. First we identified reflection events, which is helpful for us to verify our prediction results. We also created a numerical finite-difference acoustic model using the same parameters as our physical model. We set the boundary conditions to be absorbing for all sides, which means there are no free-surface multiples in the synthetic data. We calculated the two-way travel times for primaries and multiples (1<sup>st</sup> order internal multiples and 1<sup>st</sup> order free-surface multiples). The expected time is approximate because of the measurement error associated with the thickness of each block, and the water depth. In Figure 5, the interpretations are illustrated. Events A, B, D, E are primaries and C, F, H, J are first-order internal multiples. The two events G and I are first-order free-surface multiples. The approximate travel time of each event is listed in Table 2.

We also compare the zero-offset trace from the synthetic data against the zero-offset trace from physical modeling data. Figure 6a is the zero-offset trace from the physical modeling data, alongside which in Figure 6b the synthetic data zero-offset trace is plotted. Note that the two traces are not exactly identical, as there are some phase, amplitude as well as travel time differences between the two traces. These are within the expected variability caused by non-welded contact between the various slabs (Mahmoudian, 2013), evaporation over time in the tank, and measurements of each slab's thickness. Within this expected variability we conclude that the synthetic and physical modeling data match.

The ray paths for the internal multiples labelled IM1 through IM4 are illustrated in Figure 7. Note that there are two superimposed events labelled peg-leg multiple IM2, which have different paths but the same arrival times.

### Internal multiple prediction

The formula for 1.5D internal multiple prediction (Weglein et al., 1997; 2003) is

$$\begin{aligned} \text{PRED}(k_g, \omega) = & \int_{-\infty}^{\infty} dz e^{ik_z z} b_1(k_g, z) \int_{-\infty}^{z-\epsilon} dz' e^{-ik_z z'} b_1(k_g, z') \\ & \times \int_{z'+\epsilon}^{\infty} dz'' e^{ik_z z''} b_1(k_g, z'') \end{aligned}$$

where  $k_z = 2q_g$  and the  $q_g = \frac{\omega}{c_0} \sqrt{1 - \frac{k_g^2 c_0^2}{\omega^2}}$  is the vertical wavenumber associated with the lateral wavenumber  $k_g$ , the reference velocity  $c_0$  and the temporal frequency  $\omega$ . The quantity  $b_1$  is the input to the prediction algorithm.

The prediction process is applied to the physical modeling data. The SEGY file of physical modeling data was loaded into the prediction algorithm. The data are transformed from the space/time domain to the wavenumber/pseudo-depth domain to create the input  $b_1(k_g, z)$ . The quantity  $z = c_0 * t/2$  is the pseudo-depth defined in terms of reference P-wave velocity  $c_0$  and vertical travel time  $t$ . After the construction of the input, the 1.5D algorithm, which can be thought of as a sequence of 1D internal multiple

predictions, one per output  $k_g$  value, is run. An  $\epsilon$  value, whose practical importance was first pointed out by Coates and Weglein (1996) is chosen based on the width of the wavelet. Effects of various  $\epsilon$  values have been described in Pan and Innanen (2014), which showed that a smaller  $\epsilon$  value will result in far-offset artifacts at the arrival time of primaries. Meanwhile, a larger  $\epsilon$  value will damage the prediction output at near offsets. Here we determine the optimal  $\epsilon$  value to be 80 sample points.

An important issue is raised by the notable absence in the prediction of internal multiples generated within the aluminum slab. The aluminum slab has a velocity of 6000m/s and a thickness of 132m which means the two reflections generated by the aluminum slab are very close to each other. Our internal multiple prediction relies on events being separated in time by at least the  $\epsilon$  value, which is 80ms in this case. The two-way travel time for the top of the aluminum slab is about 1.861s and about 1.905s for the bottom, which means they are separated by 44ms. Since this is within the time interval rejected by  $\epsilon = 80$ ms, these two events will not be considered subevents, and the associated internal multiple will be neglected in the prediction.

The internal multiple algorithm is designed assuming free-surface multiples have been removed (Weglein et al., 1997). Thus, the free-surface multiple events in our data set should be expected to cause artifacts also, since the prediction algorithm will assume the free-surface multiple events to be primaries. In our case the free-surface multiples at sufficiently late times in the shot record, which means spurious predictions will not appear until times later than those we currently analyze. For this reason free-surface multiple removal, nominally a significant step in pre-processing, can be safely avoided in our study.

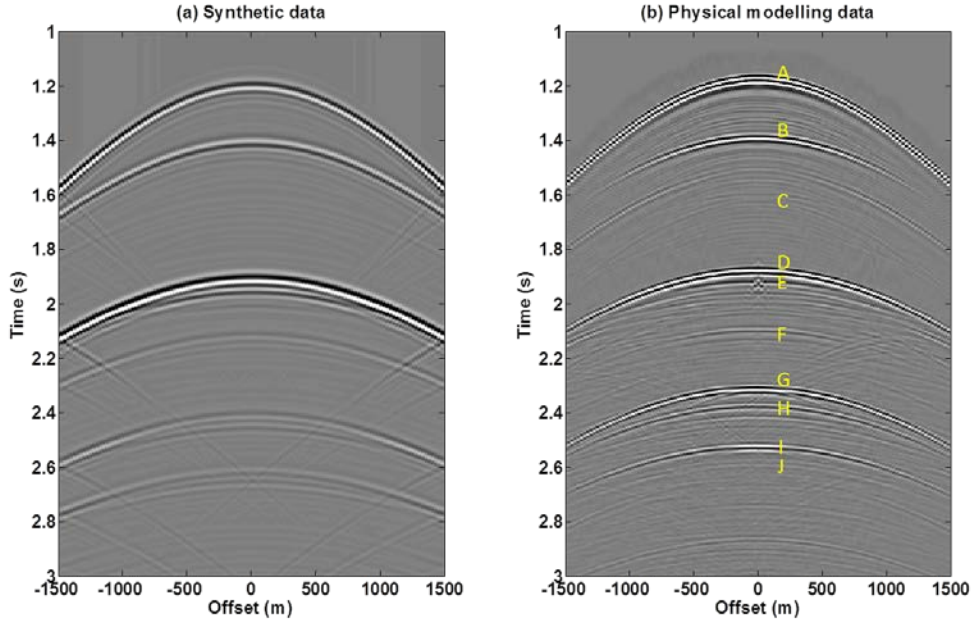


FIG. 5. Event identification by calculating two-way travel times. Reflection events are labeled on the physical modeling data set. (a) Synthetic data using the same parameters as physical modeling data; (b) physical modeling data.

Table 2. Summary of approximate travel times of the identified events.

LABEL	EVENT	APPROXIMATE TRAVEL TIME
A	Top of PVC slab	1.155s
B	Bottom of PVC slab	1.365s
C	Internal multiple 1	1.575s
D	Top of aluminum slab	1.861s
E	Bottom of aluminum slab	1.905s
F	Internal multiple 2	2.071s
G	Free-surface multiple	2.31s
H	Internal multiple 3	2.357s
I	Free-surface multiple	2.52s
J	Internal multiple 4	2.567s

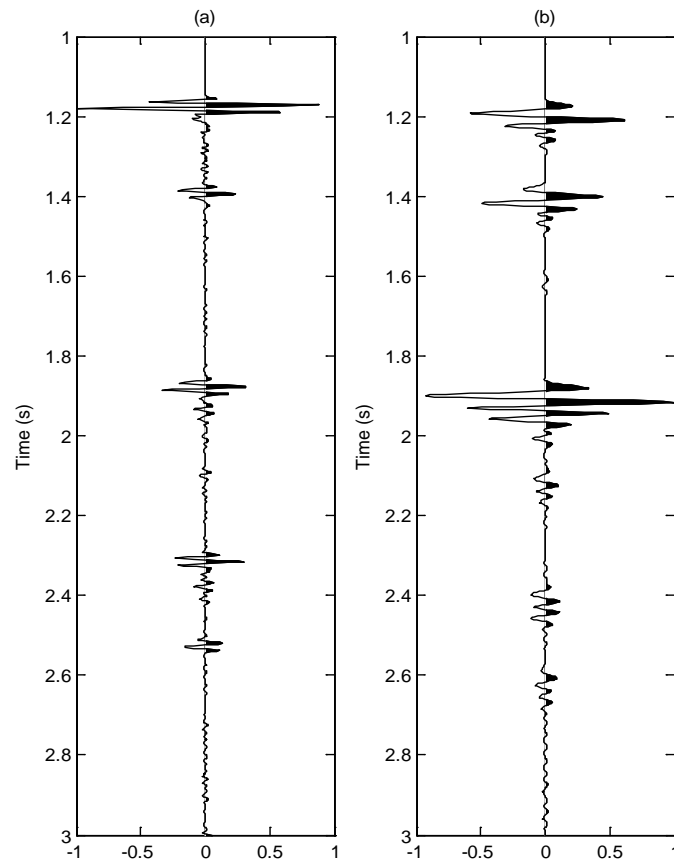


FIG. 6. Zero-offset trace from physical modeling data vs. zero-offset trace from synthetic data. (a) The physical modeling trace; (b) the synthetic data trace.

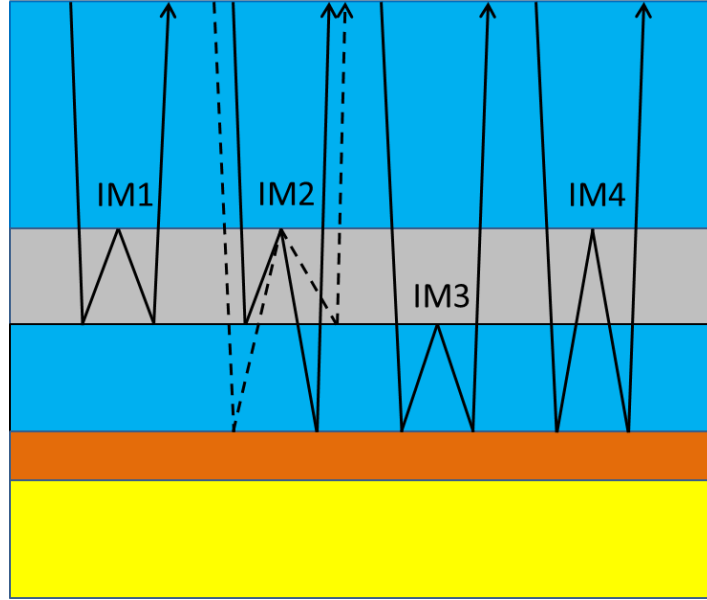


FIG. 7. The ray paths of the four dominant internal multiples expected from the physical model. Note that M2 consist of two peg-leg paths, whose travel times are identical.

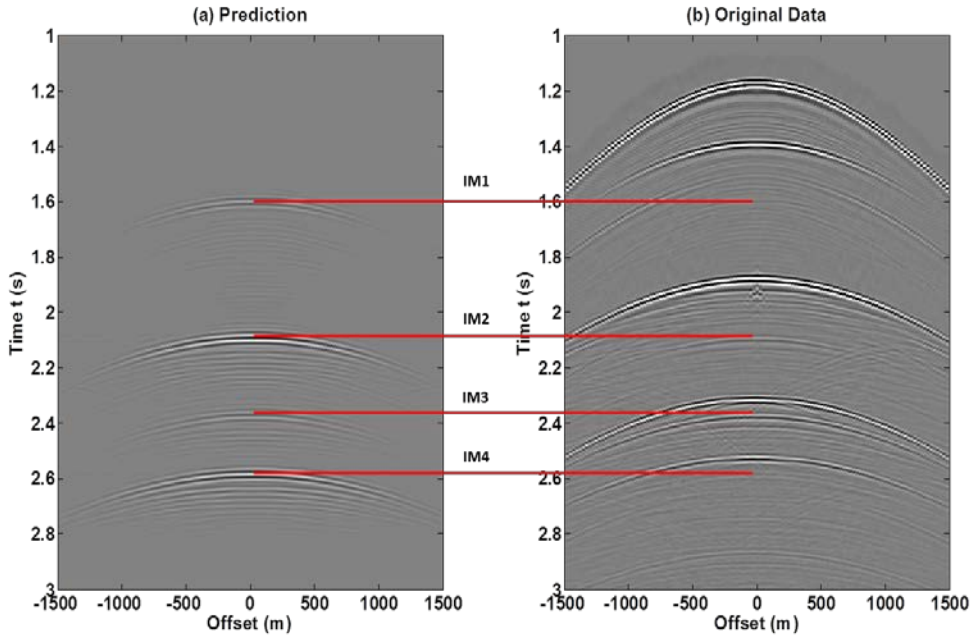


FIG. 8. Comparison of prediction output with input. (a) Prediction output; (b) input data. The red lines indicate the positions of internal multiples in both input and output data.

Figure 8a is the prediction output, with its events labeled in comparison to the physical modeling data in Figure 8b. The red lines indicate the positions of internal multiples in both input and output data. The labels on the internal multiples are consistent with Figure 7. The prediction and the physical modeling data are in good agreement. Artifacts in the form of near-offset oscillations from missing lateral wavenumber combinations (with

some influence of the noise in the physical modeling data) are visible. The zero offset trace from this output is also examined in detail in Figure 9. The zero offset trace from the physical modeling data is plotted in Figure 9a, the prediction output in Figure 9b, and the zero offset trace from the synthetic data is plotted for comparison in Figure 9c. Even though there are some non-negligible artifacts below each predicted internal multiple, arrival times of the prediction and the synthetic data match well.

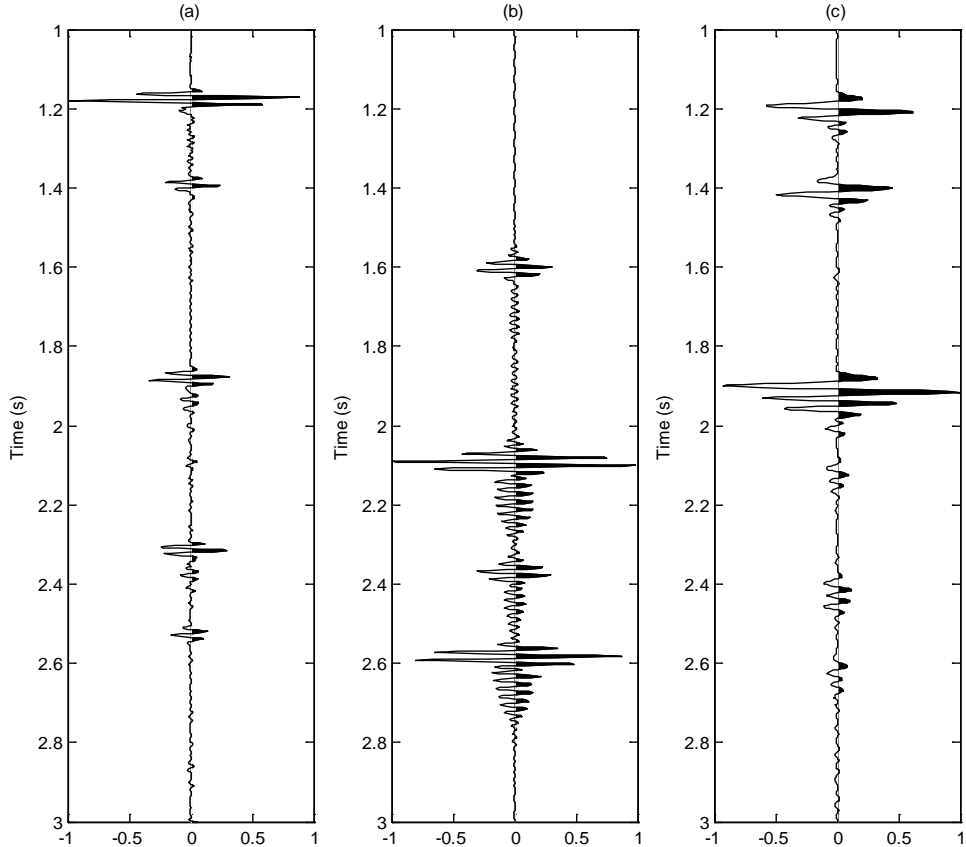


FIG. 9. Detail of internal multiple prediction. (a) Input trace (zero offset trace from the physical modeling data); (b) prediction output (zero offset trace from the prediction output in Figure 8); (c) zero offset trace from synthetic data.

### Analysis of the three parameters chosen in the algorithm

The 1.5D prediction algorithm contains three nested loops over lateral wavenumber, frequency, and pseudo depth. In this section, we perform an analysis of different chosen beginning and ending integration points. Beginning and ending integration points in the nested integrals can be chosen optimally to reduce computational burden (Innanen, 2012). Selecting frequencies properly not only affects computational cost but also quality of the final image. In Figure 10, we illustrate two prediction frequencies of 10-50Hz and 30-80Hz respectively. We can see that in Figure 10a there is a lot of noise above and below each internal multiple event, while in Figure 10b the data is much cleaner. The

frequencies can be chosen optimally from a simple Fourier decibel spectrum (Figure 11) as the 30 to 80Hz range seems to contain the desired data. The rest of the data is buried in the noise.

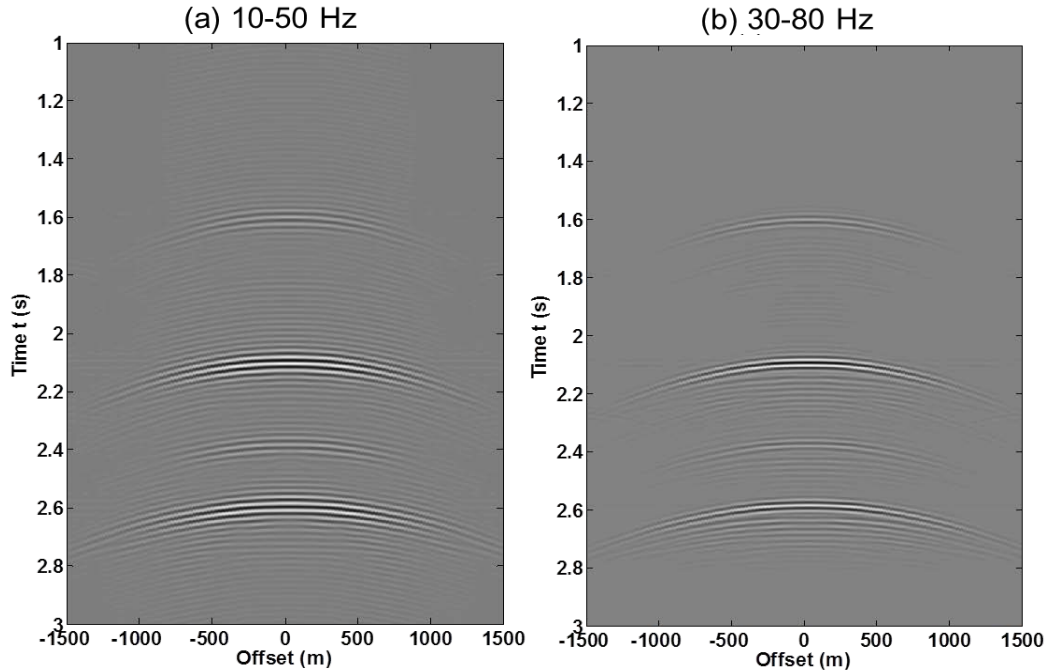


FIG. 10. Comparison of two internal multiple prediction outputs with different maximum and minimum frequencies chosen. (a) 10-50 Hz; (b) 30-80 Hz.

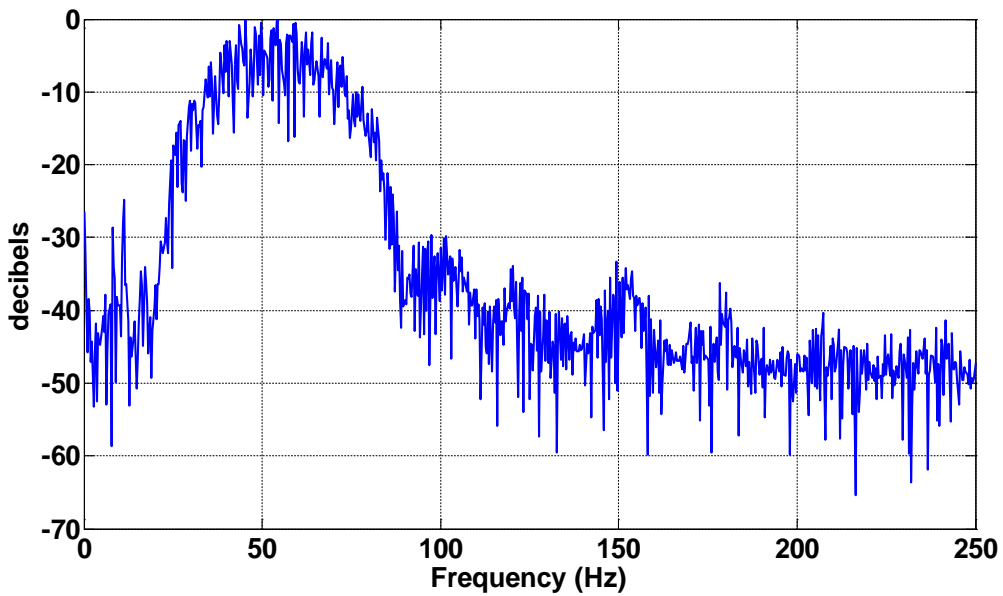


FIG. 11. Fourier amplitude spectrum of the zero-offset trace using a decibel scale.

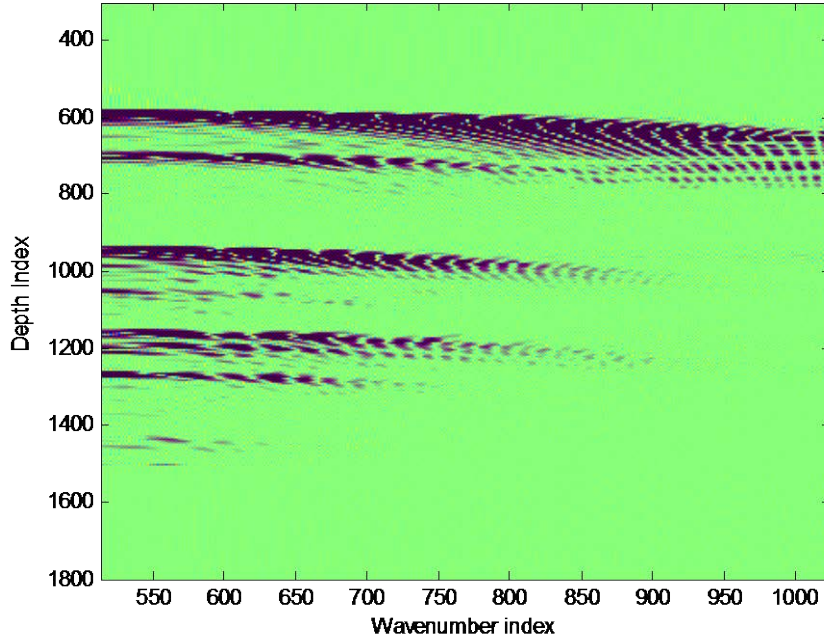


FIG. 12. The algorithm input  $b_1(k_g, z)$  is generated using the input data and the single reference velocity  $c_0$ . Note this is only one side of the data, later through conjugate symmetry the wavenumbers on the other side are filled.

Table 3. Time costs with different parameters chosen.

freBEG (Hz)	freEND (Hz)	zBEG	zEND	kxBEG	kxEND	Time (s)
25	80	540	1020	513	1024	1256.96
25	80	560	1015	513	1024	1189.85
25	80	560	1015	513	900	856.57
25	80	560	1015	513	800	636.24
30	80	560	1015	513	800	588.51

From Figure 12 we can determine that the shallowest contribution comes from depth index 540 and last contribution primary is roughly 1020. By the same principle we chose the smallest and largest contributing wavenumber indexes to be 513 and 1024. We can choose these parameters by an iterative procedure, in which depth and wavenumber index ranges are gradually narrowed down until it reaches the points that will not destroy the final image. In Table 3 we illustrate a series of experiments that shows considerable computational savings by manipulating the parameters. We compare the final result with the first experiment, which shows a time cost savings of 114%.

## CONCLUSIONS

We examine a MATLAB implementation of the 1.5D version of the inverse scattering series internal multiple prediction algorithm on marine physical modeling seismic data. We use ProMax to pre-process the data to suppress reverberations between the first two primaries. Deconvolution and deghosting are important steps in pre-processing. In the physical model experiment, the source and receiver transducers are very close to the water surface, so we do not expect strong source or receiver ghosts, and the deghosting step can be avoided. We also build a synthetic data set using a finite-difference program for comparison. Prediction results show good agreement with both synthetic data and physical modeling data. The effect on the algorithm of the choice of a single  $\epsilon$  value is also discussed. Even if subtraction is problematic, prediction results can lead us to obtain an “internal multiple probability map”, useful for identifying both internal multiples and primaries whose amplitudes are likely to have experienced interference from them. However, it is also true that even a simple variable  $\epsilon(k_g)$  may provide significantly improved prediction results permitting subtraction to proceed. Choosing the beginning and ending integration points in the nested integrals optimally leads to considerable computation savings.

## ACKNOWLEDGEMENTS

This work was funded by CREWES. We would like to thank the sponsors of CREWES for the financial support. Thank you to Kevin Bertram, who was a great help with physical modeling experiment and David Hanley for helping with the pre-processing using ProMax.

## REFERENCES

- Coates, R. T., and Weglein, A. B., 1996, Internal multiple attenuation using inverse scattering: Results from prestack 1D and 2D acoustic and elastic synthetics: 66<sup>th</sup> Annual International Meeting, SEG, Expanded Abstracts, 1522-1525.
- Geldart, L.P., and Sheriff, R.E., 2004, Problems in Exploration Seismology and their solutions: Society of Exploration Geophysicists, p. 332.
- Hernandez, M., and Innanen, K. A., 2014, Identifying internal multiples using 1D prediction: physical modelling and land data examples, Canadian Journal of Geophysical Exploration, **39**, 1, 37-47.
- Innanen, K. A., 2012, 1.5D internal multiple prediction in MATLAB: CREWES Annual Report, **24**, No. 35, 1-7.
- Lawton, D.C., Cheadle, S.P., Gallant, E.V., and Bertram, M.B., 1989, Elastic physical modeling: CREWES Research Report, **1**, No. 19, 273-288.
- Lawton, D.C., Margrave, G.F., and Gallant, E.V., 1998, Physical modeling of an anisotropic thrust, CREWES Research Report, **10**, No. 15, 1-9.
- Mahmoudian, F., 2013, Physical modeling and analysis of seismic data from a simulated fractured medium: PhD Thesis, University of Calgary.
- Pan, P., and Innanen, K. A., 2014, Numerical analysis of 1.5D internal multiple prediction: 84th Annual International Meeting, SEG, Expanded Abstracts, 4135-4139.

Reshef, M., Keydar, S., and Landa, E., 2003, Multiple prediction without pre stack data - an efficient tool for interpretive processing: *First Break*, **21**, No. 3.

Weglein, A. B., F. V. Araújo, P. M. Carvalho, R. H. Stolt, K. H. Matson, R. T. Coates, D. Corrigan, D. J. Foster, S. A. Shaw, and H. Zhang, 2003, Inverse scattering series and seismic exploration: *Inverse Problems*, **19**, R27-R83.

Weglein, A. B., Gasparotto, F. A., Carvalho, P. M., and Stolt, R. H., 1997, An inverse-scattering series method for attenuating multiples in seismic reflection data: *Geophysics*, **62**, No. 6, 1975–1989.

Wong, J., Maier, R., Gallant, E.V., and Lawton, D.C., 2009a, Physical modeling of a 3D marine seismic survey: *CREWES Research Report*, **21**, No. 74, 1-10.

Wong, J., Hall, K.W., Gallant, E.V., Maier, R., Bertram, M.B., Lawton, D.C., 2009b, Seismic Physical Modelling at the University of Calgary, *CSEG Recorder*, **34**, p. 37-43.